








## RESEARCH ARTICLE

# Pectin methylesterification state and cell wall mechanical properties contribute to neighbor proximity-induced hypocotyl growth in *Arabidopsis*

Fabien Sénéchal<sup>1</sup>  | Sarah Robinson<sup>2</sup>  | Evert Van Schaik<sup>3</sup>  |  
 Martine Trévisan<sup>1</sup>  | Prashant Saxena<sup>1</sup>  | Didier Reinhardt<sup>3</sup>  |  
 Christian Fankhauser<sup>1</sup> 

<sup>1</sup>Centre for Integrative Genomics, Faculty of Biology and Medicine, Géopode Building, University of Lausanne, Lausanne, Switzerland

<sup>2</sup>Institute of Plant Sciences, University of Bern, Bern, Switzerland

<sup>3</sup>Department of Biology, University of Fribourg, Fribourg, Switzerland

## Correspondence

Fabien Sénéchal, UMR INRAE 1158 BioEcoAgro, Plant Biology and Innovation, University of Picardie Jules Verne, Amiens, France.  
 Email: [fabien.senechal@u-picardie.fr](mailto:fabien.senechal@u-picardie.fr)

## Present addresses

Fabien Sénéchal, UMR INRAE 1158 BioEcoAgro, Plant Biology and Innovation, University of Picardie Jules Verne, Amiens, France; Sarah Robinson, The Sainsbury Laboratory, University of Cambridge, Cambridge, UK; Evert Van Schaik, University of Applied Sciences Leiden, Leiden, Netherlands; and Prashant Saxena, James Watt School of Engineering, University of Glasgow, Glasgow, UK.

## Funding information

This work was supported by the grant “Plant Growth 2 in a Changing Environment” funded by the Swiss initiative in systems biology (SystemX.ch) to Cris Kuhlemeier (Bern), Didier Reinhardt (Fribourg), and Christian Fankhauser (Lausanne). Work in the Fankhauser lab was supported by the University of Lausanne and the Swiss National Science Foundation (grant 310030B\_179558).

## Abstract

Plants growing with neighbors compete for light and consequently increase the growth of their vegetative organs to enhance access to sunlight. This response, called shade avoidance syndrome (SAS), involves photoreceptors such as phytochromes as well as phytochrome interacting factors (PIFs), which regulate the expression of growth-mediating genes. Numerous cell wall-related genes belong to the putative targets of PIFs, and the importance of cell wall modifications for enabling growth was extensively shown in developmental models such as dark-grown hypocotyl. However, the contribution of the cell wall in the growth of de-etiolated seedlings regulated by shade cues remains poorly established. Through analyses of mechanical and biochemical properties of the cell wall coupled with transcriptomic analysis of cell wall-related genes from previously published data, we provide evidence suggesting that cell wall modifications are important for neighbor proximity-induced elongation. Further analysis using loss-of-function mutants impaired in the synthesis and remodeling of the main cell wall polymers corroborated this. We focused on the *cgr2cgr3* double mutant that is defective in methylesterification of homogalacturonan (HG)-type pectins. By following hypocotyl growth kinetically and spatially and analyzing the mechanical and biochemical properties of cell walls, we found that methylesterification of HG-type pectins was required to enable global cell wall modifications underlying neighbor proximity-induced hypocotyl growth. Collectively, our work suggests that plant competition for light induces changes in the expression of numerous cell wall genes to enable modifications in biochemical and mechanical properties of cell walls that contribute to neighbor proximity-induced growth.

This is an open access article under the terms of the [Creative Commons Attribution-NonCommercial-NoDerivs](https://creativecommons.org/licenses/by-nc-nd/4.0/) License, which permits use and distribution in any medium, provided the original work is properly cited, the use is non-commercial and no modifications or adaptations are made.

© 2024 The Authors. *Plant Direct* published by American Society of Plant Biologists and the Society for Experimental Biology and John Wiley & Sons Ltd.

## 1 | INTRODUCTION

Plants growing in dense populations compete for light required for photosynthesis (Fiorucci & Fankhauser, 2017). The proximity of competitors and shade are perceived as a change in light intensity and quality, resulting in various developmental adaptations (Galvão & Fankhauser, 2015). Depending on their response to shade, plants are classified into shade-tolerant and shade-avoiding species (Gommers et al., 2013). The latter react to shade with characteristic growth responses in order to reach full sunlight for photosynthesis. This phenomenon, known as shade avoidance syndrome (SAS) can be observed in most aerial organs and involves a range of developmental changes (Pierik & De Wit, 2014). For example, SAS entails early flowering and inhibition of branching, leaves adopt an upright position (hyponasty), and petioles, stems, and hypocotyls elongate (de Wit et al., 2016). These changes accelerate the life cycle of plants and warrant survival and propagation under limited light availability.

The phytochrome (phy) type photoreceptors have a central role in SAS with phyB playing a predominant role in *Arabidopsis thaliana* (Legris et al., 2019). Under high Red:Far Red (R:FR) conditions, corresponding to full sunlight, active phyB moves into the nucleus, where it interacts with transcription factors known as phytochrome interacting factors (PIFs) to inhibit their activities. Low R:FR conditions, on the other hand, cause inactivation of phyB and derepression of the PIFs, which modulate genes required for shade-induced growth (de Wit et al., 2016). A central mechanism in shade-induced growth is auxin biosynthesis in cotyledons and young leaves followed by polar transport and distribution in hypocotyls and stems, which elongate in response to shade (de Wit et al., 2014). phyB and PIFs also act locally in the hypocotyl to promote growth through mechanisms that are less clearly established (Fiorucci & Fankhauser, 2017; Pucciariello et al., 2018). For example, PIFs regulate the expression of genes required for plasma-membrane lipid biogenesis in the hypocotyl (Ince et al., 2022). Moreover, numerous genes encoding cell wall-modifying proteins are induced by shade and targeted by PIFs (Kohnen et al., 2016; Pedmale et al., 2016), suggesting the role of cell wall metabolism in the establishment of shade-regulated growth.

The primary cell wall of growing plant organs has seemingly contradictory functions. On the one hand, it provides mechanical strength to maintain cell shape and plant stature, on the other hand, it has to remain elastic and plastic to allow cell expansion and plant growth (Bashline et al., 2014). In dicotyledonous species such as *Arabidopsis*, the primary cell wall consists of interconnected networks of polysaccharides and structural proteins/glycoproteins (Cosgrove, 2005; Nguema-Ona et al., 2014; Wolf, Hématy, & Höfte, 2012). A first network of cellulose microfibrils cross-linked by hemicelluloses (Network 1) is embedded in a second network made by pectins that have gelling properties (Network 2). Pectins are intimately associated with a third network (Network 3), consisting mainly of glycoproteins such as extensins (EXTs) and arabinogalactan proteins (AGPs) (Hijazi et al., 2014). This complex three-dimensional mesh resists internal turgor pressure, and at the same time, yields to allow cell growth. Dynamic adjustment of physical cell wall properties (e.g., stiffness,

elasticity, and plasticity) involves cell wall-synthesizing and modifying enzymes that usually belong to multigenic families and constantly modulate cell walls to allow growth (Atmodjo et al., 2013; Pauly & Keegstra, 2016; Sénéchal, Wattier, et al., 2014; Showalter & Basu, 2016).

Cell wall remodeling plays a central role in the control of seedling development, however, its contribution to adaptive growth phenomena in response to environmental cues such as SAS remains poorly understood. Although transcriptomic analyses suggested that cell wall remodeling may play a central role in adaptive growth processes (Kohnen et al., 2016), direct functional evidence is scarce. A role for xyloglucans in SAS has been established for petiole elongation in *Arabidopsis* (Sasidharan et al., 2010; Sasidharan & Pierik, 2010), and for shade-induced growth in *Stellaria longipes* (Sasidharan et al., 2008). Here, we took a systematic approach to explore the contribution of cell wall remodeling in SAS of the *Arabidopsis* hypocotyl. By combining Fourier-transform infrared (FTIR) analyses of cell wall constituents with measurements of cell wall biophysics, we show that cell wall remodeling is triggered at early stages of the growth response induced by low R:FR, indicative of neighbor proximity that is a form of SAS. Employing systematic transcriptomic and genetic analysis with mutants affected in various aspects of cell wall biosynthesis and modification, we establish pectin methylesterification status as a determinant of cell wall extensibility in the neighbor proximity-induced hypocotyl growth.

## 2 | RESULTS

### 2.1 | Low R:FR induces cell elongation mainly in the middle part of the hypocotyl

In order to simulate the proximity of competing neighbors, we subjected *Arabidopsis* seedlings to white light supplemented with far red (low R:FR ratio). Within 1 day, this led to increased hypocotyl growth compared with control seedlings kept in white light (high R:FR ratio) (Figure S1). In order to determine the site of growth, we used the borders of epidermal cells as marks because hypocotyl elongation proceeds almost exclusively by cell elongation without cell division. In order to assess cell dimensions, confocal images of seedlings were segmented in MorphoGraphX (de Reuille et al., 2015), followed by semiautomated cell size measurements. Cell length along the length of the hypocotyl was increased by low R:FR primarily in the middle part of the hypocotyl (Figure 1).

### 2.2 | Low R:FR changes mechanical properties of hypocotyl cell walls

To assess the mechanical properties of the hypocotyl during growth induced by low R:FR, we used an automated confocal micro-extensometer (ACME, Robinson et al., 2017). This approach enabled in vivo quantification of the elastic properties of cell walls. Hypocotyls

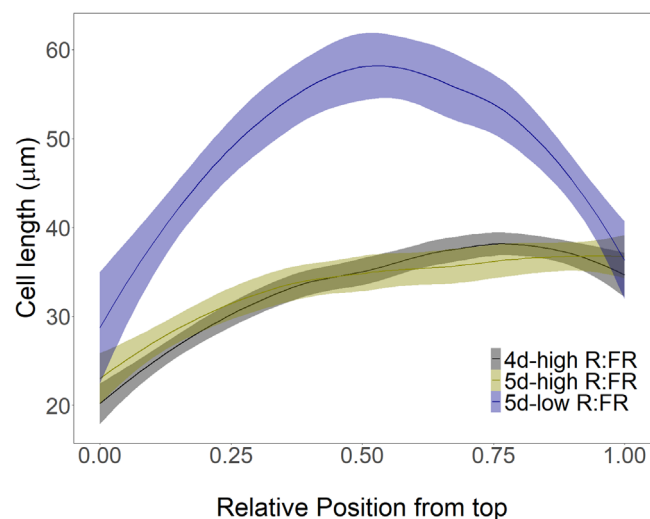


**FIGURE 1** Low R:FR induces fast growth in the middle part of the hypocotyl. Length of the hypocotyl epidermis cells in response to high and low R:FR treatments. After 4 days under high R:FR (black curve), Col-0 seedlings were grown for 1 day under high R:FR (yellow curve) or low R:FR (blue curve). The length of the epidermis cells was plotted from the top to the bottom part of the hypocotyl. The curves show means in  $\mu\text{m} \pm$  confidence intervals (shaded areas).

of intact seedlings were abraded by freezing and thawing and subjected to repeated cycles of application and removal of 5 mN of force. Our analysis revealed increased strain under low R:FR after 1 day of treatment and decreased strain after 3 days (Figure 2a). Interestingly, this effect was specific to low R:FR conditions because no such changes were observed under high R:FR (Figure 2a).

To relate growth and mechanical changes induced by low R:FR to cell wall properties, we applied FTIR microspectroscopy to cells located in the middle part of the hypocotyl. The relative absorbance intensities for wavelengths related to the cell wall (from 830 to 1800  $\text{cm}^{-1}$ ) were selected to assess the composition and status of various cell wall polysaccharides. FTIR analysis revealed significantly different patterns of relative absorption induced by low R:FR ratio after 3 days of treatment (Figures 2b and S2). The main differences were observed between 1530 and 1200  $\text{cm}^{-1}$  and between 1180 and 1030  $\text{cm}^{-1}$  (Figure 2b). A relative decrease (at 1740 and between 1530 and 1200  $\text{cm}^{-1}$ ) suggests lower levels of pectins and xyloglucans, as well as cellulose and lignin. On the other hand, an increase between 1180 and 1030  $\text{cm}^{-1}$  rather indicates enrichment of pectins, xyloglucans, cellulose, and arabinogalactan that can relate both to AGPs and rhamnogalacturonan I-type pectins (Figure 2b). These results indicate major cell wall modifications in response to low R:FR ratio. In order to obtain further insight into the changed cell wall components, we performed hierarchical clustering for the wavelengths that have previously been assigned to certain cell wall components (Alonso-simón et al., 2011; Kakuráková et al., 2000; Largo-Gosens et al., 2014; Mouille et al., 2003; Szymanska-Chargot & Zdunek, 2013; Wilson et al., 2000) (Figure 2c). This data was consistent with an overall enrichment for pectins with a low degree of methylesterification

(DM, de-esterified pectins), in addition to other pectins, AGPs, cellulose, and xyloglucans in response to low R:FR, while other wavelengths assigned to pectins, cellulose, and xyloglucans showed opposite trends. Depending on the chemical bonds revealed by the wavelengths, different structural parts of the polysaccharides could be assessed such as backbone and side chains. This may explain opposite trends for wavelengths related to the same polysaccharide, which can be more abundant with reduced side chains for instance. Taken together, these results are consistent with major changes in cell wall biosynthesis and remodeling in response to low R:FR.

### 2.3 | Low R:FR impinges on expression of cell wall-related genes

In order to investigate transcriptional regulation of cell wall properties under low R:FR, we considered 40 gene families that are thought to be involved in the synthesis and/or remodeling of cell wall components. The expression of a total of 824 genes was analyzed using an RNA sequencing dataset, previously published, and coming from a time course experiment under low R:FR conditions (Kohnen et al., 2016). In this set of genes, 544 were found to be expressed in seedlings grown under control conditions, among which 224 were regulated by low R:FR in hypocotyls (Figure 3a). Only few genes were regulated in cotyledons or in both organs (26 and 16 genes, respectively) (Figure 3a). Most genes were regulated at later stages (90 or 180 min after the onset of light stimulus), and they were mostly up-regulated, in particular in hypocotyls (Figure 3a). Modulated genes comprised functions related to (hemi)cellulose (Network 1), pectin (Network 2), and structural proteins (Network 3) (Figure 3b). The few genes that were induced at the early time points (15 or 45 min after the onset of the light stimulus) in hypocotyls are involved in cell wall remodeling: At1g49490:EXT, At5g47500:PME (pectin methyltransferase), At1g62760:PMEI (PME inhibitor), At5g02260:EXP (expansin), At5g57560:XTH (xyloglucan endotransglucosidase hydrolase), At1g02405:EXT, and At3g10710:PME (Tables S1A,B). Considering the global influence of FR light on cell biosynthetic genes, the highest percentage related to pectins (Network 2) with 96% of the genes expressed in seedlings, and 52% affected by low R:FR conditions. Especially, numerous genes encoding homogalacturonan (HG) synthesizing enzymes are upregulated in the hypocotyl of low R:FR treated seedlings, such as galacturonosyltransferases (GAUTs, 11/15 genes), GAUT-like (GATL, 6/10 genes), and HG methyltransferases (HGMTs, 5/7 genes) (Table S1A,B). Taken together, these results suggest that cell wall remodeling is initiated within the first 15 min of low R:FR treatment, followed by general cell wall modifications involving both synthesis and remodeling of all cell wall constituents, in particular of HG-type pectin.

SAS is controlled by PIFs, hence, we interrogated previously published chromatin immunoprecipitation (ChIP) sequencing data (Kohnen et al., 2016) for binding to PIF4 and PIF5 with the 224 genes regulated in the hypocotyl under low R:FR conditions. This revealed that 59 genes are putative direct PIF4 and/or PIF5 targets (Figure S3

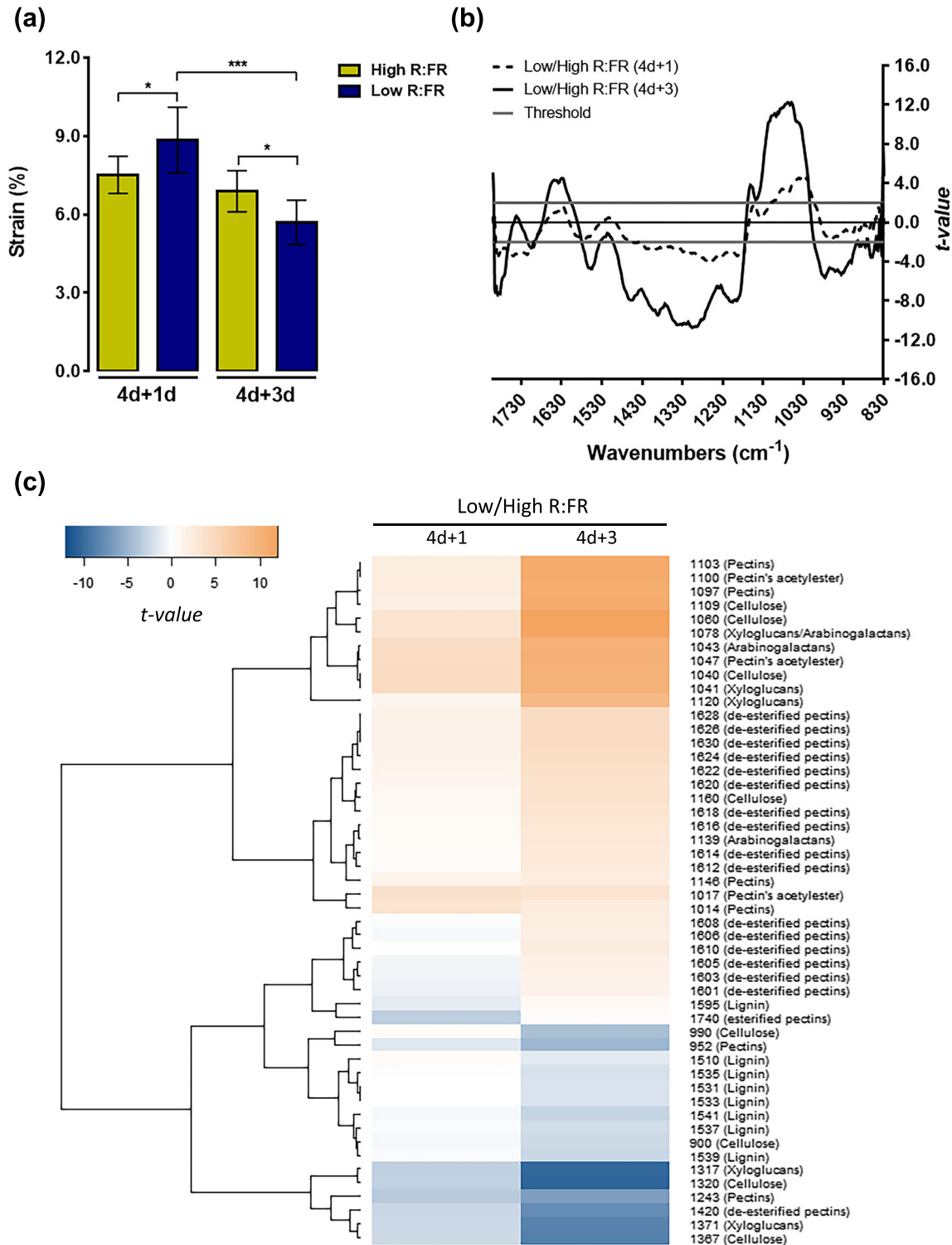


FIGURE 2 Legend on next page.

**FIGURE 2** Low R:FR induces changes in mechanical and cell wall properties of the hypocotyl. (a) Elastic properties of hypocotyl assessed under high and low R:FR treatment. Hypocotyls were frozen and thawed then subjected to cycles of application and removal of 5 mN of force using an automated confocal micro extensometer (see Section 4). The average magnitude of strain incurred by seedlings grown in a high R:FR (yellow bars) or low R:FR (blue bars) light regime after 1 (4 days + 1 day) and 3 days (4 days + 3 days) is shown. Bright-field images were collected every 645 ms and strain was computed from regions that were tracked in the images using the automated confocal micro-extensometer (ACME) tracker software. The bars show means in  $\% \pm SD$  ( $n > 10$  independent seedlings, at least five oscillations were made). Pairwise comparisons were made using Welch *t*-test brackets indicated statistical tests that were made with significance  $p < .1^*$ ,  $p < .05^{**}$ , and  $p < .01^{***}$ . (b, c) Cell wall properties in the middle part of the hypocotyl under high and low R:FR treatments. Cell wall chemical bounds were analyzed by Fourier-transform infrared (FTIR) microspectroscopy. For each hypocotyl, six spectra were collected in the middle part, avoiding the central cylinder, for at least five independent hypocotyls per condition. Baseline correction and data normalization were made for the absorbances between 1810 and 830  $\text{cm}^{-1}$  (corresponding to the cell wall fingerprint, see Figure S1). Pairwise comparison between high and low R:FR was made after 1 and 3 days of treatments and significant differences were identified using Student's *t*-test for each wavelength. (b) All Student's *t*-values were plotted against wavelengths with horizontal lines referring to the significant threshold for  $p < .05$ . Student's *t*-values above +2 or below -2 indicate, respectively, an enrichment or an impoverishment of cell wall components in low compared with high R:FR. (c) Student's *t*-values for wavelengths assigned to cell wall components were used to build the heatmap with negative and positive *t*-values, respectively, represented by a range of colors from blue to orange.

and Table S1C), including genes related to all three polymer networks, as well as to all processes including cell wall synthesis, remodeling, and signaling. Despite genes encoding HG biosynthetic enzymes seem especially upregulated by low R:FR treatment, a limited number of genes for *GAUTs* (1/15 genes), *HGMTs* (2/7 genes), and to a lesser extent for *GATLs* (5/10 genes) were identified as potential PIF4 and/or PIF5 target genes (Table S1C). This suggests direct and indirect regulations of genes encoding HG biosynthetic enzymes by PIF transcription factors.

## 2.4 | Cell wall-related mutants reveal the role of cell wall components in low R:FR-induced growth

In order to gain insight into the mechanisms involved in low R:FR-induced growth, loss-of-function mutants defective in the three networks (cellulose, pectin, and glycoproteins) were investigated for growth phenotypes under low R:FR treatment (Table S2, Figure 4a). We selected *xxt* mutants impaired in xyloglucan biosynthesis (Network 1), mutants affected in pectin biosynthesis (*gaut*, *gat1*, and *cgr*) and pectin remodeling (*pme* and *pmei*; Network 2), and mutants affected in AGP biosynthesis (*galt*, *agp10c*, and *fla9*; Network 3). While most of the mutants did not have noticeable hypocotyl length phenotypes after 4 days under high R:FR, some of them showed increased hypocotyl length and hypocotyl length was slightly reduced in the *xxt1xxt5* mutant (Figure S4). A slight shift in the germination time between wild type and mutants can produce differences in hypocotyl length measured at Day 4. Thus, all of these mutants were subjected to low R:FR treatment for 3 days, from Days 4 to 7, and their hypocotyl growth response was measured and normalized to their respective wild types (Figure 4a). None of the single mutants in Network 1 had a growth phenotype, possibly because of genetic redundancy, but the double mutants *xxt1xxt2* and *xxt2xxt5* showed significantly reduced hypocotyl elongation in response to low R:FR. In Network 2 mutants, only *cgr2* had a growth defect, which was exacerbated in the *cgr2cgr3* double mutant. Unexpectedly, mutants affected in Network 3 generally grew longer than the wild type. Taken

together, these results highlight the importance of xyloglucan and pectin in SAS, while some proteinaceous components of the cell walls appear to restrict hypocotyl elongation in the wild type.

Based (i) on the induction of several *HGMTs* by low R:FR treatment (Figure S5), including the previously characterized *HGMT* genes *CGR2* and *CGR3* (Kim et al., 2015), (ii) on the putative regulation of *CGR3* by PIF4 and PIF5 previously identified through ChIP sequencing analysis (Figure S3, Table S1C; Kohlen et al., 2016), and (iii) on the strong growth phenotype of the *cgr2cgr3* double mutant (Figure 4a), we investigated cell wall constituents in *cgr2cgr3* by FTIR analyses using wavelengths assigned to methylesterified (1740  $\text{cm}^{-1}$ ) and demethylesterified (1630  $\text{cm}^{-1}$ ) pectins (Figure S6). Using these wavelengths, we estimated the DM, which was decreased by approximately 40% in *cgr2cgr3* compared with the wild type. In a time course experiment, *cgr2cgr3* was not affected in hypocotyl growth under control conditions (high R:FR), however, under low R:FR conditions, growth was reduced (Figure 4b). In particular, *cgr2cgr3* reacted slower (4 days + 1 day) and weaker (4 days + 3 days) than the wild type (Figure 4b). The growth defect of *cgr2cgr3* was particularly pronounced in the middle part of the hypocotyl which normally shows the strongest growth response (Figure S7). This indicates that *cgr2cgr3* mutants have a defect in low R:FR-induced epidermal cell elongation.

We next assessed the mechanical properties of *cgr2cgr3* hypocotyls in response to low R:FR (Figure 4c). Wild-type hypocotyls had shown an increase in cell wall strain after 1 day, and a decrease after 3 days of FR treatment (Figure 2a). In contrast, *cgr2cgr3* did not show a change in strain at either time point, possibly indicating that cell wall remodeling is defective in the double mutant. To further address this aspect, we investigated the cell wall composition of *cgr2cgr3* by FTIR microspectroscopy as in the wild type (Figure 2b,c), in the range of wavelengths from 830 to 1800  $\text{cm}^{-1}$  to obtain a cell wall fingerprint. This analysis was performed in the middle part of hypocotyls which shows the strongest growth increment under low R:FR (Figures 1 and S8). Relative absorbances for Col-0 and *cgr2cgr3* did not show significant changes in response to low R:FR after the first day (Figures 5a and S8A,B upper panels). However, 3 days after transfer, both wild

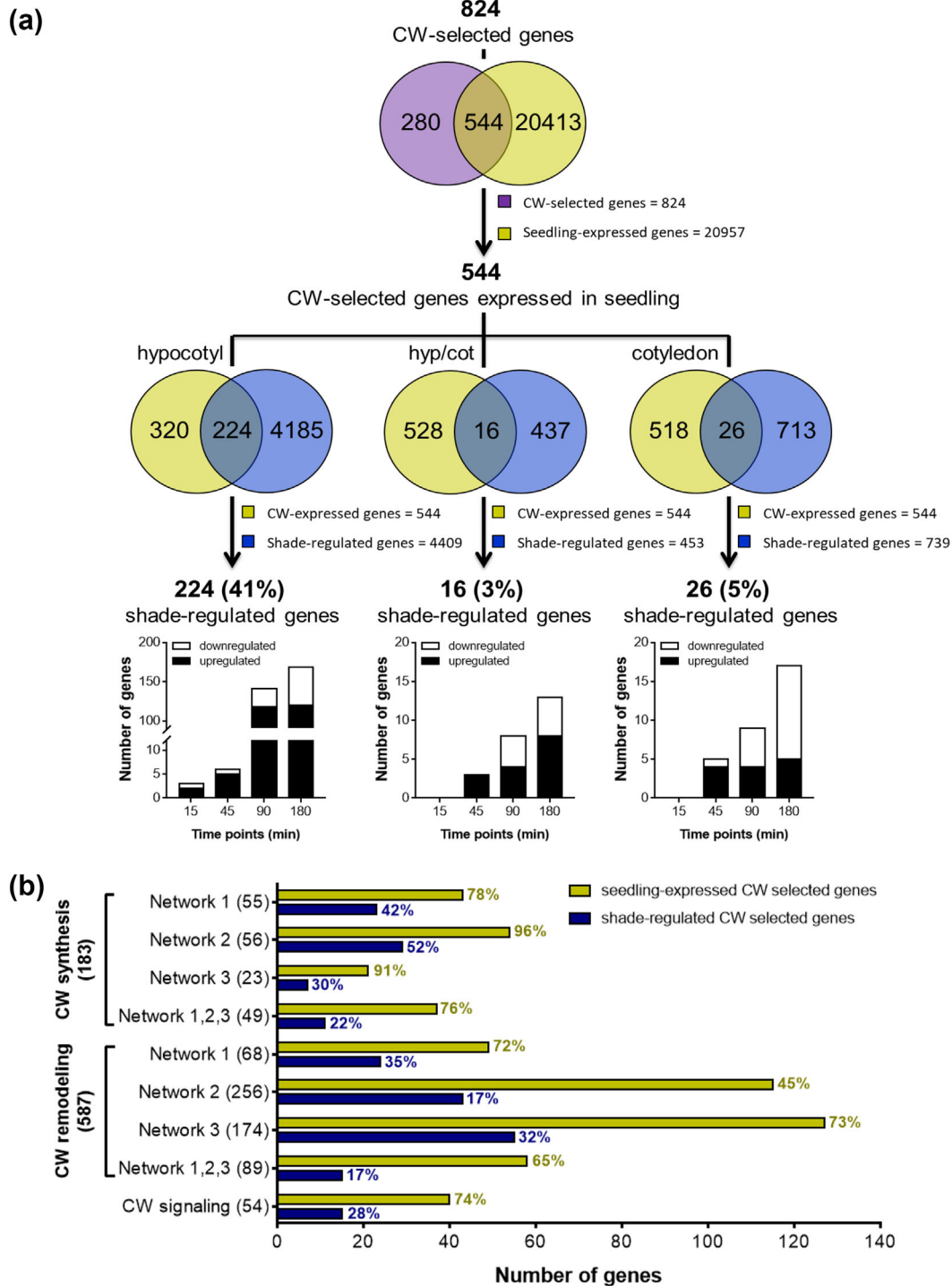


**FIGURE 3** Low R:FR triggers changes in the expression of cell wall-related genes. (a) Number of cell wall-related genes identified as expressed in seedling and regulated by low R:FR in hypocotyl, cotyledon or both. From cell wall-selected genes and RNA sequencing data (Kohnen et al., 2016), Venn diagrams highlight cell wall-related genes expressed in seedling and that are regulated by low R:FR in hypocotyl, cotyledon or both. For each, a number of up and down-regulated genes are shown along the kinetic of low R:FR treatment. Percentages of the low R:FR-regulated genes were determined according to the total of cell wall-related genes expressed in seedling. (b) Number of cell wall-related genes expressed in seedling and regulated by low R:FR classified according to their putative function in cell wall synthesis, remodeling, and signaling as well as their related networks for synthesis and remodeling. Percentages were determined according to the total of cell wall-related genes classified for each condition (values between brackets). CW, cell wall; Network 1, cellulose and hemicelluloses; Network 2, pectins; Network 3, structural proteins.

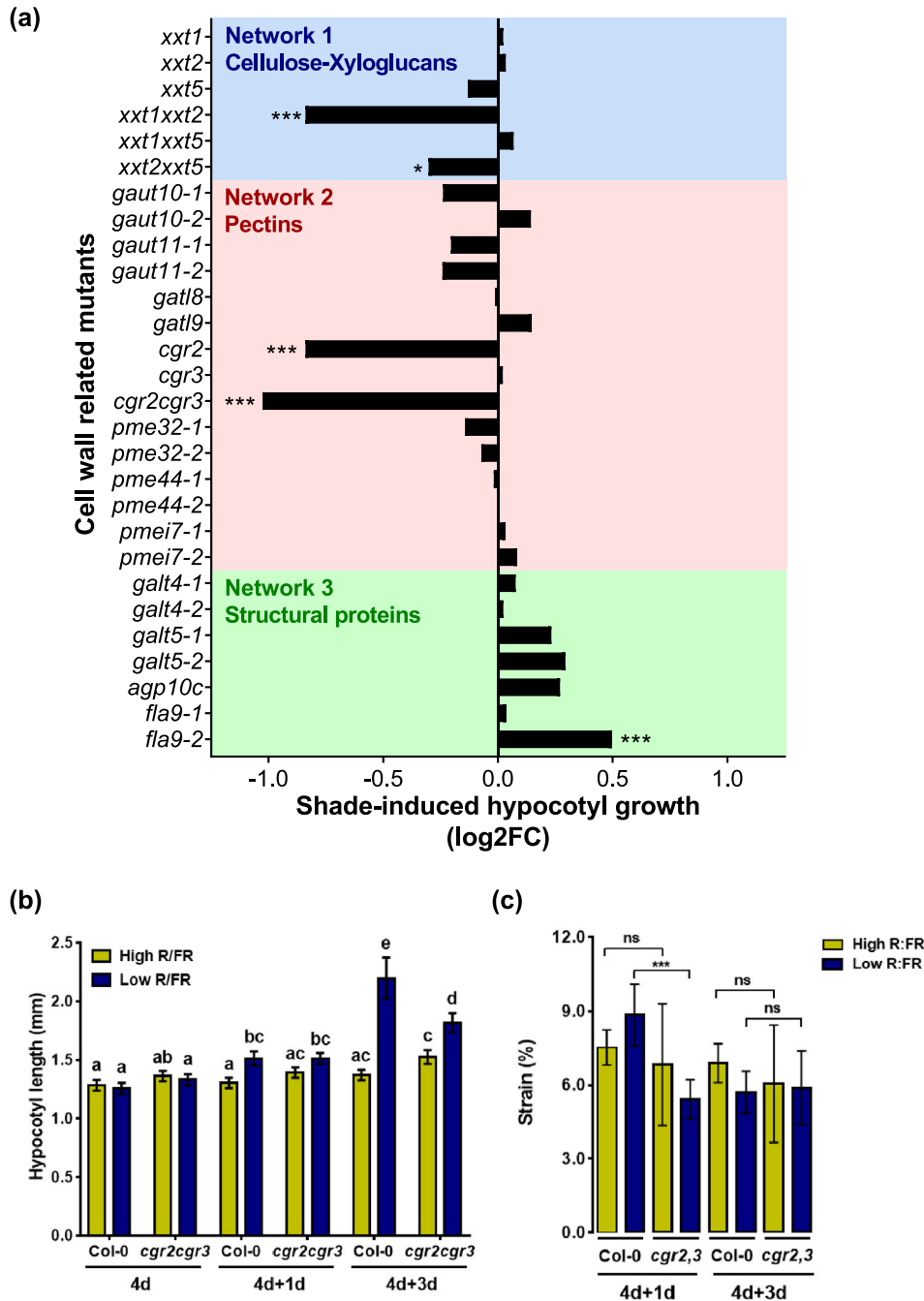


**FIGURE 4** Analysis of mutants impaired in cell wall metabolism reveals the importance of CGR2 and CGR3 in the regulation of the hypocotyl growth and the elastic properties under low R:FR. (a) Length of the hypocotyls in response to low R:FR treatment. Seedlings were grown for 4 days in high R:FR and then for three additional days in low R:FR. Data of growth induced by low R:FR during the 3 days were normalized against the wild type and expressed in log<sub>2</sub>FC. Significant differences ( $p < .05^*$ ,  $p < .001^{***}$ ) were determined according to Student's *t*-test. (b) Length of the hypocotyls in response to high and low R:FR treatments in Col-0 and *cgr2cgr3*. Seedlings were grown for 4 days in high R:FR before being transferred under low R:FR (blue bars) or kept in high R:FR (yellow bars) for three additional days. The bars show means in mm  $\pm$  confidence intervals measured at 4 (4 days), 5 (4 days + 1 day), and 7 (4 days + 3 days) days. Significant differences (indicated with letters) were determined according to one-way ANOVA followed by multiple comparisons with Tukey's test. (c) Elastic properties of hypocotyl assessed under high and low R:FR treatment for Col-0 and *cgr2cgr3*. Hypocotyls were frozen and thawed then subjected to cyclic loading at 5 mN of force and the strain compared with the data obtained for the wild-type seedlings in Figure 2. The average magnitude of strain incurred by seedlings grown in a high R:FR or low R:FR light regime after 1 (4 days + 1 day) and 3 days (4 days + 3 days) is shown. The bars show means in %  $\pm$  SD ( $n > 10$  independent seedlings for Col-0 and  $n > 5$  independent seedlings for *cgr2cgr3*, at least five oscillations were made per seedling). Pairwise comparisons were made between the mutant and the wild-type using Welch *t*-test brackets indicated statistical tests that were made with significance  $p < .1^*$ ,  $p < .05^{**}$ , and  $p < .01^{***}$ .

type and *cgr2cgr3* showed significant changes in relative absorbances in response to low R:FR conditions (Figures 5a and S8A,B, lower panels). Overall, the pattern of the significantly affected wavelengths was similar for both genotypes, but the differences were more pronounced in the wild type than in *cgr2cgr3* (Figure 5b).

The main differences between the genotypes were observed in the range of wavelengths from 1630 to 1500  $\text{cm}^{-1}$  with a significant decrease in relative absorbances in the wild type but not in *cgr2cgr3* (Figure 5b), and from 1180 to 1030  $\text{cm}^{-1}$ , where the wild type showed a stronger increase in relative absorbances than the double mutant. These results suggest that a change in pectin methylesterification in *cgr2cgr3* may result in secondary changes in cell wall composition (Figure 5b).

### 3 | DISCUSSION

While growth is simple to quantify, in particular in an organ like the hypocotyl that grows essentially in only one dimension, the underlying molecular mechanisms are extremely complex because they involve multiple regulatory levels such as hormonal and metabolic regulation, transcriptional activation of growth-related genes, and ultimately remodeling of the complex three-dimensional cell wall polymer network. Thanks to the ease of mutational analysis of growth, many of the upstream regulatory components in SAS have been identified (Ballaré & Pierik, 2017; Fiorucci & Fankhauser, 2017; Procko et al., 2014). A reduced R:FR indicative of neighbor proximity is primarily perceived by phyB in cotyledons and young leaves (Ballaré & Pierik, 2017; Fiorucci & Fankhauser, 2017). This leads to PIF-mediated induction of auxin production, which following transport to the hypocotyl promotes elongation (Ballaré & Pierik, 2017; Fiorucci & Fankhauser, 2017; Procko et al., 2014). PIFs can also directly regulate the expression of hypocotyl specific genes as shown for genes encoding enzymes involved in plasma-membrane biogenesis (Ince et al., 2022). Our expression analysis, from previously published RNA seq. data (Kohnen et al., 2016), suggests low R:FR induces extensive hypocotyl-specific regulation of genes encoding enzymes involved in cell wall biosynthesis and remodeling (Figure 3), which ultimately results in alteration of cell wall properties and induction of growth. However, due to the interdependency of cell wall components, it has been difficult to disentangle the role of individual cell wall components in growth. Here, we identified and characterized pectin methylesterification status as an important element in the growth phenomenon of Arabidopsis seedlings in the shade avoidance response.

Pectin consists mainly of HG which represents a linear polymer of galacturonic acid (GalA) synthesized by GAUT and GATL enzymes in the Golgi apparatus (Atmodjo et al., 2013). HG is subsequently methylesterified by HGMTs before secretion into the cell wall, where it can be selectively demethylesterified by PME (Sénéchal, Wattier, et al., 2014). Thus, PME activity adjusts the DM, which in turn modulates cell wall mechanical properties (Peaucelle et al., 2011; Wang et al., 2020). Furthermore, PME-mediated demethylesterification can

expose HG to pectin-degrading enzymes such as polygalacturonases (PGs) and pectate lyases-like (PLLs) (Sénéchal, Wattier, et al., 2014). Pectin degradation by these enzymes can contribute to cell wall loosening. There is evidence for a functional role of pectin metabolism in the regulation of growth (Bouton, 2002; Guénin et al., 2011; Mouille et al., 2007; Pelletier et al., 2010; Rui et al., 2017; Sénéchal, Graff, et al., 2014; Wang et al., 2010; Wolf, Mravec, et al., 2012; Xiao et al., 2014), however, the high degree of redundancy in cell-wall remodeling enzymes has complicated the analysis. For example, there are 66 and 76 genes, respectively, that encode PMEs and PMEIs, allowing for extensive compensatory responses upon genetic or pharmacological interference.

A mechanistic understanding of growth phenomena requires the combined use of genetic, analytic, and biomechanical methods to identify the causal elements in cell growth. Using FTIR analysis, we document changes in cell wall composition in response to changes in the R:FR ratio, which correlate with accelerated growth. We identified two HGMT genes (*CGR2* and *CGR3*) that are required for neighbor proximity-induced growth. Biomechanical assays showed that *CGR2* and *CGR3* might contribute to cell wall extensibility at the onset of growth. Previous studies used atomic force microscopy to analyze cell walls, which measure properties perpendicular to the direction of growth, to detect differences in mechanical properties in plants with modified pectin that correlated with growth (Braybrook & Peaucelle, 2013; Peaucelle et al., 2008; Peaucelle et al., 2011; Peaucelle et al., 2015). In this study, we were able to measure differences in mechanical properties using an extensometer which measures properties in the direction of growth. Both approaches show a correlation between modifying pectin chemistry, changes in cell wall mechanical properties and growth, supporting the role of pectin in growth regulation. Further work is required to understand the nature of this regulation and how it relates to the other cell wall components (Coen & Cosgrove, 2023).

Taken together, our results highlight the contribution of pectin methylesterification during neighbor proximity-induced hypocotyl growth. Moreover, our data suggests that changes in cell wall chemical composition and mechanical properties are important for hypocotyl growth regulation. However, further investigations are required to identify the chemical and mechanical features causally linked to neighbor-proximity-induced hypocotyl growth promotion.

## 4 | MATERIALS AND METHODS

### 4.1 | Plant material and growth conditions

*A. thaliana* Columbia (Col-0) and Wassilewskija (Ws) ecotypes were used. A set of cell wall-related mutants was used for investigating cell wall metabolism under shade-induced growth. Some of these mutants were provided by research groups that have previously characterized them, while others were ordered from NASC (Table S2). All of these mutants were PCR-genotyped using oligonucleotides listed in Table S3.



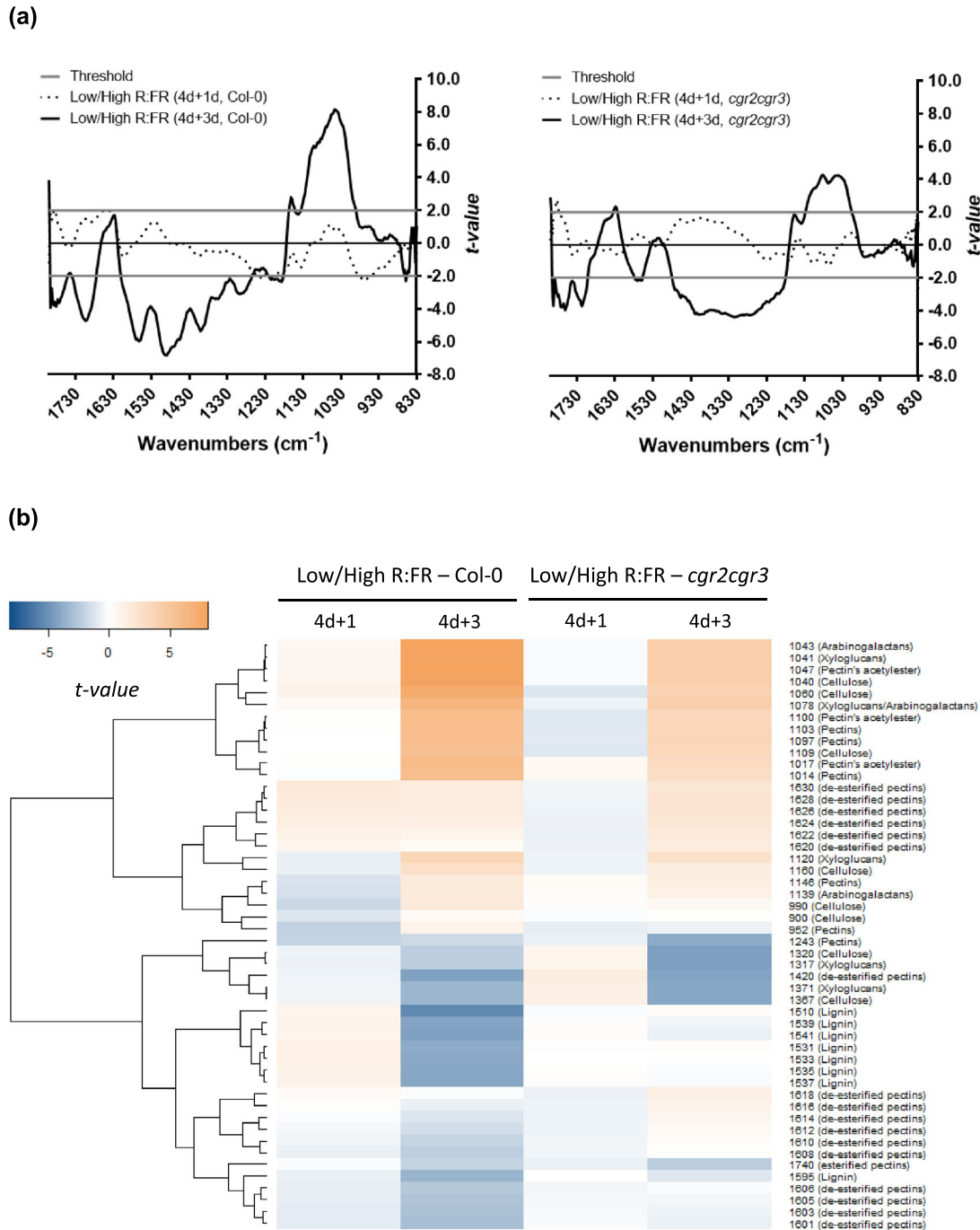


**FIGURE 5** Changes of cell wall properties that occur in response to low R:FR are reduced in *cgr2cgr3*. (a, b) Cell wall properties in the middle part of the hypocotyl under high and low R:FR treatments for Col-0 and *cgr2cgr3*. Cell wall chemical bounds were analyzed by Fourier-transform infrared (FTIR) microspectroscopy. For each hypocotyl, six spectra were collected in the middle part, avoiding the central cylinder, for at least five independent hypocotyls per condition. Baseline correction and data normalization were made for the absorbances between 1810 and 830  $\text{cm}^{-1}$  (corresponding to the cell wall fingerprint, see Figure S6). Pairwise comparison between high and low R:FR was made after 1 and 3 days of treatments for Col-0 and *cgr2cgr3* and significant differences were identified using Student's *t*-test for each wavelength. (a) All Student's *t*-values were plotted against wavelengths with horizontal lines referring to the significant threshold for  $p < .05$  for Col-0 (left panel) and *cgr2cgr3* (right panel). Student's *t*-values above +2 or below -2 indicate, respectively, an enrichment or an impoverishment of cell wall components in low compared with high R:FR. (b) Student's *t*-values for wavelengths assigned to cell wall components were used to build the heatmap with negative and positive *t*-values, respectively, represented by a range of colors from blue to orange.

The method for seed sterilization and stratification as well as the composition of the growth media were previously described (Kohnen et al., 2016). Seedlings were grown on vertical plates at 21°C in a long

day photoperiod (16 h light/8 h dark) in a growth cabinet (AR22L, Percival) in constant white light (photosynthetically active radiation (PAR)  $\sim 110 \mu\text{mol}/\text{m}^2/\text{s}$ ). For reproducing conditions that relate to

neighbor proximity, seedlings were grown for 4 days in high R:FR condition (R:FR  $\sim$ 10), then subsequently transferred under low R:FR (R:FR  $\sim$ 0.1) or kept in high R:FR as a control, for additional 3 days. The composition of the light spectrum in the growth cabinet was measured following the method previously described (Dornbusch et al., 2012) and allowed calculation of the R:FR ratio. Pictures were taken on Day 4, as well as Days 5 and 7 and length of hypocotyls was measured using semi-automated MATLAB script implemented by Dr. Prashant Saxena.

## 4.2 | Imaging and length measurement of hypocotyl epidermis cells

Seedlings used for cell length measurements were collected at various time points and light treatments then fixed on ice for 1 h with methanol (40%) and acetic acid (10%), followed by staining with calcofluor white (.1%, Tris-HCl .1 M, pH = 8.5, Mercks) for 5–14 days. A minimum of seven hypocotyls were imaged per treatment. Confocal pictures were taken with a Leica TCS SP5. Sample staining was emitted with a diode laser: 405 nm. The gain was adjusted to signal. Z-stacks were taken with a maximum distance of the pixel size. Image analyses were done using the MorphoGraphX software with adapted protocols (de Reuille et al., 2014; de Reuille et al., 2015; Robinson et al., 2017).

Z-stacks were loaded in MorphoGraphX in which first the filter autoscale was applied, followed by the filter Gaussian Blur Stack (value 2  $\mu$ m). Images were then segmented using ITK Watershed Auto Seeded. Segmentations were turned into a mesh with Marching Cubes 3D with a cube size of 5  $\mu$ m and no smoothing. Segmentation at this point was checked for quality. Only properly segmented cells were used in analyses. A Bezier curve with a minimum order of five was drawn in a single cell file along the length of the hypocotyl. Shape analyses were done with PCAnalysis using elliptical cylinders. The output files were processed in R Studio using ggplot2. The cell width was calculated as the average of R2 and R3 and the cell volume was calculated as  $\text{Pi} \cdot \text{R1} \cdot \text{R2} \cdot \text{R3}$ . The averages were calculated using locally estimated scatterplot smoothing (LOESS) fitting and plotted using a .99 confidence interval. LOESS fittings were used to calculate percentile differences between curves.

## 4.3 | Determination of the mechanical properties

Mechanical properties were tested using an ACME as in Robinson et al. (2017). Seedlings grown on vertical plates and collected at various time points and light treatments were flash-frozen in liquid nitrogen. Individual seedlings were then thawed and lightly compressed with a microscope slide to remove water. Seedlings were attached to ACME using tough tags and superglue. They were then subjected to at least 5 cycles of application and removal of 5 mN of force, while submerged in distilled water. Bright-field images were collected every 645 ms. The strain was computed from regions that were tracked in the images using the ACME tracker software (Robinson et al., 2017).

## 4.4 | Cell wall analysis by Fourier-transform infrared (FTIR) microspectroscopy

Seedlings grown on vertical plates were collected at various time points and light treatments and immediately incubated in absolute ethanol for 1 week. The samples were subsequently incubated twice in 80% ethanol for 5 min at 100°C, twice in absolute acetone for 5 min at room temperature, and resuspended in water (Sénéchal, Graff, et al., 2014). Hydrated seedlings were squashed between the glass slide and the gold-coated slide. The glass slide was thereafter carefully removed and the seedlings stilled on the gold-coated slide were dried for 30 min at 37°C for infrared spectra collection.

FTIR spectroscopy was performed on a Nicolet iN 10 microscope system using the related Omnic Picta software (Thermo Scientific) on dried seedlings laid on the gold-coated slides (Mazurek et al., 2013; Mravec et al., 2017). The spectra collection was done using the following parameters: reflection mode for the collection with an aperture of 30  $\mu$ m  $\times$  30  $\mu$ m and a collection time of 96 scans/spectra at the spectral resolution of 4  $\text{cm}^{-1}$ . Absorbance was collected in a spectral range of wavelength from 400 to 4000  $\text{cm}^{-1}$ . For each condition (time point and light treatment) five to six seedlings were analyzed and for each, six spectra were collected in the middle part of hypocotyl, avoiding the central cylinder. Collected data were normalized and baseline corrected using an R script provided by Dr. Gregory Mouille (Mouille et al., 2003), then averaged for hypocotyls of the same condition. In the range from 830 to 1800  $\text{cm}^{-1}$  that corresponds to the cell wall fingerprint, results were statistically analyzed and plotted with relative absorbance or t-value for each wavelength (505 wavelength values from 830 to 1800  $\text{cm}^{-1}$ ). Additionally, t-values for wavelengths assigned to cell wall components were hierarchically clustered using a heatmap, built with gplots package on R software. Assignment of wavelength to cell wall component was done using research articles and reviews related to FTIR spectroscopy and cell wall chemistry (Alonso-simón et al., 2011; Kakuráková et al., 2000; Largo-Gosens et al., 2014; Mouille et al., 2003; Szymanska-Chargot & Zdunek, 2013; Wilson et al., 2000).

The DM of pectins was estimated with calculation using absorbance intensities of the wavelengths 1630 and 1740  $\text{cm}^{-1}$ , respectively, assigned to the de-esterified and esterified pectins and the equation previously described:  $\text{DM} = \frac{A_{1740}}{A_{1740} + A_{1630}} \times 100$  (Leroux et al., 2015). This method for measuring DM with FTIR data was validated with various commercial substrates of chemically known DM (Leroux et al., 2015).

## 4.5 | Analyses of published RNA and ChIP sequencing data

Using The Arabidopsis Information Resource (TAIR) (<https://www.arabidopsis.org/>) and carbohydrate-active enzymes database (CAZy) (<http://www.cazy.org/>) online databases, 824 putative cell wall-related genes were selected for analysis of their expression in response to low R:FR using previously published RNA sequencing



data (Kohnen et al., 2016). According to their genome annotation and biochemical characterization, for some of them, these genes were classified into various families with subdivision by cell wall network and synthesis or remodeling features as well as signaling for gene encoding cell wall receptors (Tables S1A and S4).

The same set of genes was used for comparing genes encoding cell wall proteins that are modulated by low R:FR and putatively targeted by PIF4 and/or PIF5. Thus, the genes identified as modulated by low R:FR in hypocotyl were compared with CHIP sequencing data for PIF4 (Oh et al., 2012) and PIF5 (Hornitschek et al., 2012) that were reanalyzed (Kohnen et al., 2016) following a pipeline previously described (Heyndrickx et al., 2014). From this comparison, a Venn diagram was made on the Bioinformatics and Evolutionary Genomics website (<http://bioinformatics.psb.ugent.be/webtools/Venn/>).

#### 4.6 | Statistical analysis

For hypocotyl length comparisons, significant differences were determined using one-way ANOVA followed by multiple comparisons of means using Tukey's or Dunnett's post hoc test. In the case where comparisons were made between every data group, letters indicate significance for a  $p$ -value  $< .05$ . In the case where comparisons were made according to a specific control, significances are indicated with \* for  $p$ -value  $< .05$ , \*\* for  $p$ -value  $< .01$ , and \*\*\*  $p$ -value  $< .001$ . For pairwise comparisons of mechanical properties, the Welch  $t$ -test was used with significant differences indicated with \* for  $p$ -value  $< .05$ , \*\* for  $p$ -value  $< .01$ , and \*\*\* for  $p$ -value  $< .001$ . For pairwise comparisons of FTIR data groups, Student's  $t$ -test was made using relative absorbance for each wavelength and  $t$ -values were plotted. Differences are significant when  $t$ -values are upper or lower than the threshold of +2 and -2, respectively.

#### AUTHOR CONTRIBUTIONS

**Conceptualization:** Christian Fankhauser, Didier Reinhardt, Fabien Sénéchal, Sarah Robinson, and Evert Van Schaik. **Formal analysis:** Fabien Sénéchal, Sarah Robinson, Evert Van Schaik, Martine Trévisan, and Prashant Saxena. **Funding acquisition:** Christian Fankhauser and Didier Reinhardt. **Investigation:** Fabien Sénéchal, Sarah Robinson, Evert Van Schaik, Martine Trévisan, and Prashant Saxena. **Project administration:** Christian Fankhauser and Didier Reinhardt. **Software:** Prashant Saxena, Sarah Robinson, Fabien Sénéchal, and Evert Van Schaik. **Validation:** Fabien Sénéchal, Sarah Robinson, Evert Van Schaik, Christian Fankhauser, and Didier Reinhardt. **Visualization:** Fabien Sénéchal, Sarah Robinson, and Evert Van Schaik. **Supervision:** Christian Fankhauser and Didier Reinhardt. **Writing—original draft preparation:** Fabien Sénéchal, Sarah Robinson, and Evert Van Schaik. **Writing—review and editing:** Fabien Sénéchal, Sarah Robinson, Didier Reinhardt, and Christian Fankhauser.

#### ACKNOWLEDGMENTS

The authors wish to gratefully thank Prof. Kenneth Keegstra, Prof. Debra Mohnen, Prof. Federica Brandizzi, and Prof. Jérôme Pelloux,

respectively, for sharing seeds of the *xxt*, *gaut*, *cgr*, and *pme/pmei* mutants used in this study. We also thank Dr. Christiane Nawrath, Dr. Sylvester Mazurek, and Dr. Gregory Mouille for their help in the analysis of the FTIR microspectroscopy. We thank the Swiss initiative in systems biology (SystemX.ch) and the University of Lausanne for the funding support. We nicely thank Prof. Cris Kuhlemeier for contributing to the funding acquisition and the co-supervising of the “Plant Growth 2 in a Changing Environment” project funded by the Swiss initiative in systems biology (SystemX.ch). We also thank him for his help in the project handling and for hosting Sarah Robinson, a postdoc in his lab during the project.


#### CONFLICT OF INTEREST STATEMENT

The authors did not report any conflict of interest.

#### DATA AVAILABILITY STATEMENT

All data used in the manuscript are presented in the main figures and supplementary data. Raw data are available from the authors upon request, and for transcriptomic analyses in Kohnen et al. (2016) (<https://doi.org/10.1105/tpc.16.00463>).

#### ORCID

Fabien Sénéchal  <https://orcid.org/0000-0002-4145-7205>  
 Sarah Robinson  <https://orcid.org/0000-0001-7643-1059>  
 Evert Van Schaik  <https://orcid.org/0009-0008-9475-0393>  
 Martine Trévisan  <https://orcid.org/0000-0002-6610-6954>  
 Prashant Saxena  <https://orcid.org/0000-0001-5071-726X>  
 Didier Reinhardt  <https://orcid.org/0000-0003-3495-6783>  
 Christian Fankhauser  <https://orcid.org/0000-0003-4719-5901>

#### REFERENCES

- Alonso-simón, A., García-angulo, P., Mérida, H., Encina, A., Álvarez, J. M., & Acebes, J. L. (2011). The use of FTIR spectroscopy to monitor modifications in plant cell wall architecture caused by cellulose biosynthesis inhibitors. *Plant Signaling & Behavior*, 6, 1104–1110. <https://doi.org/10.4161/psb.6.8.15793>
- Atmodjo, M. A., Hao, Z., & Mohnen, D. (2013). Evolving views of pectin biosynthesis. *Annual Review of Plant Biology*, 64, 747–779. <https://doi.org/10.1146/annurev-arplant-042811-105534>
- Ballaré, C. L., & Pierik, R. (2017). The shade-avoidance syndrome: Multiple signals and ecological consequences. *Plant, Cell & Environment*, 40, 2530–2543. <https://doi.org/10.1111/pce.12914>
- Bashline, L., Lei, L., Li, S., & Gu, Y. (2014). Cell wall, cytoskeleton, and cell expansion in higher plants. *Molecular Plant*, 7, 586–600. <https://doi.org/10.1093/mp/ssu018>
- Bouton, S. (2002). QUASIMODO1 encodes a putative membrane-bound glycosyltransferase required for normal pectin synthesis and cell adhesion in Arabidopsis. *Plant Cell Online*, 14, 2577–2590. <https://doi.org/10.1105/tpc.004259>
- Braybrook, S. A., & Peaucelle, A. (2013). Mechano-chemical aspects of organ formation in *Arabidopsis thaliana*: The relationship between auxin and pectin. *PLoS ONE*, 8, e57813. <https://doi.org/10.1371/journal.pone.0057813>
- Coen, E., & Cosgrove, D. J. (2023). The mechanics of plant morphogenesis. *Science*, 379, eade8055. <https://doi.org/10.1126/science.ade8055>
- Cosgrove, D. J. (2005). Growth of the plant cell wall. *Nature Reviews. Molecular Cell Biology*, 6, 850–861. <https://doi.org/10.1038/nrm1746>

- de Reuille, P. B., Robinson, S., & Smith, R. S. (2014). Quantifying cell shape and gene expression in the shoot apical meristem using MorphoGraphX. *Methods in Molecular Biology*, 1080, 121–134. [https://doi.org/10.1007/978-1-62703-643-6\\_10](https://doi.org/10.1007/978-1-62703-643-6_10)
- de Reuille, P. B., Routier-Kierzkowska, A. L., Kierzkowski, D., Bassel, G. W., Schüpbach, T., Tauriello, G., Bajpai, N., Strauss, S., Weber, A., Kiss, A., et al. (2015). MorphoGraphX: A platform for quantifying morphogenesis in 4D. *eLife*, 4, 1–20.
- de Wit, M., Galvão, V. C., & Fankhauser, C. (2016). Light-mediated hormonal regulation of plant growth and development. *Annual Review of Plant Biology*, 67, 513–537. <https://doi.org/10.1146/annurev-arplant-043015-112252>
- de Wit, M., Lorrain, S., & Fankhauser, C. (2014). Auxin-mediated plant architectural changes in response to shade and high temperature. *Physiologia Plantarum*, 151(1), 13–24. <https://doi.org/10.1111/ppl.12099>
- Dornbusch, T., Lorrain, S., Kuznetsov, D., Fortier, A., Liechti, R., Xenarios, I., & Fankhauser, C. (2012). Measuring the diurnal pattern of leaf hyponasty and growth in *Arabidopsis*—A novel phenotyping approach using laser scanning. *Functional Plant Biology*, 39, 860–869. <https://doi.org/10.1071/FP12018>
- Fiorucci, A. S., & Fankhauser, C. (2017). Plant strategies for enhancing access to sunlight. *Current Biology*, 27, R931–R940. <https://doi.org/10.1016/j.cub.2017.05.085>
- Galvão, V. C., & Fankhauser, C. (2015). Sensing the light environment in plants: Photoreceptors and early signaling steps. *Current Opinion in Neurobiology*, 34, 46–53. <https://doi.org/10.1016/j.conb.2015.01.013>
- Gommers, C. M. M., Visser, E. J. W., Onge, K. R. S., Voeselek, L. A. C. J., & Pierik, R. (2013). Shade tolerance: When growing tall is not an option. *Trends in Plant Science*, 18, 65–71. <https://doi.org/10.1016/j.tplants.2012.09.008>
- Guénin, S., Mareck, A., Rayon, C., Lamour, R., Assoumou Ndong, Y., Domon, J. M., Sénéchal, F., Fournet, F., Jamet, E., Canut, H., Percoco, G., Mouille, G., Rolland, A., Rustérucchi, C., Guerineau, F., van Wuytswinkel, O., Gillet, F., Driouich, A., Lerouge, P., ... Pelloux, J. (2011). Identification of pectin methylesterase 3 as a basic pectin methylesterase isoform involved in adventitious rooting in *Arabidopsis thaliana*. *The New Phytologist*, 192, 114–126. <https://doi.org/10.1111/j.1469-8137.2011.03797.x>
- Heyndrickx, K. S., de Velde, J., Van, W. C., Weigel, D., & Vandepoele, K. (2014). A functional and evolutionary perspective on transcription factor binding in *Arabidopsis thaliana*. *Plant Cell*, 26, 3894–3910. <https://doi.org/10.1105/tpc.114.130591>
- Hijazi, M., Velasquez, S. M., Jamet, E., Estevez, J. M., & Albenne, C. (2014). An update on post-translational modifications of hydroxyproline-rich glycoproteins: Toward a model highlighting their contribution to plant cell wall architecture. *Frontiers in Plant Science*, 5, 1–10. <https://doi.org/10.3389/fpls.2014.00395>
- Hornitschek, P., Kohnen, M. V., Lorrain, S., Rougemont, J., Ljung, K., López-Vidriero, I., Franco-Zorrilla, J. M., Solano, R., Trevisan, M., Pradervand, S., Xenarios, I., & Fankhauser, C. (2012). Phytochrome interacting factors 4 and 5 control seedling growth in changing light conditions by directly controlling auxin signaling. *The Plant Journal*, 71, 699–711. <https://doi.org/10.1111/j.1365-313X.2012.05033.x>
- Ince, Y. Ç., Krahmer, J., Fiorucci, A. S., Trevisan, M., Galvão, V. C., Wigger, L., Pradervand, S., Fouillen, L., Van Delft, P., Genva, M., et al. (2022). A combination of plasma membrane sterol biosynthesis and autophagy is required for shade-induced hypocotyl elongation. *Nature Communications*, 13, 5659. <https://doi.org/10.1038/s41467-022-33384-9>
- Kakuráková, M., Capek, P., Sasinkova, V., Wellner, N., Ebringerova, A., & Kac, M. (2000). FT-IR study of plant cell wall model compounds: Pectic polysaccharides and hemicelluloses. *Carbohydrate Polymers*, 43, 195–203. [https://doi.org/10.1016/S0144-8617\(00\)00151-X](https://doi.org/10.1016/S0144-8617(00)00151-X)
- Kim, S.-J., Held, M. A., Zemelis, S., Wilkerson, C., & Brandizzi, F. (2015). CGR2 and CGR3 have critical overlapping roles in pectin methylesterification and plant growth in *Arabidopsis thaliana*. *The Plant Journal*, 82, 208–220. <https://doi.org/10.1111/tpj.12802>
- Kohnen, M. V., Schmid-Siegert, E., Trevisan, M., Petrolati, L. A., Sénéchal, F., Müller-Moulé, P., Maloof, J., Xenarios, I., & Fankhauser, C. (2016). Neighbor detection induces organ-specific transcriptomes, revealing patterns underlying hypocotyl-specific growth. *Plant Cell*, 28, 2889–2904. <https://doi.org/10.1105/tpc.16.00463>
- Largo-Gosens, A., Hernández-Altamirano, M., Garcia-Calvo, L., Alonso-Simón, A., Alvarez, J., & Acebes, J. L. (2014). Fourier transform mid infrared spectroscopy applications for monitoring the structural plasticity of plant cell walls. *Frontiers in Plant Science*, 5, 1–15. <https://doi.org/10.3389/fpls.2014.00303>
- Legris, M., Ince, Y. Ç., & Fankhauser, C. (2019). Molecular mechanisms underlying phytochrome-controlled morphogenesis in plants. *Nature Communications*, 10, 5219. <https://doi.org/10.1038/s41467-019-13045-0>
- Leroux, C., Bouton, S., Kiefer-Meyer, M.-C., Fabrice, T. N., Mareck, A., Guénin, S., Fournet, F., Ringli, C., Pelloux, J., Driouich, A., Lerouge, P., Lehner, A., & Mollet, J. C. (2015). PECTIN METHYLESTERASE48 is involved in *Arabidopsis* pollen grain germination. *Plant Physiology*, 167, 367–380. <https://doi.org/10.1104/pp.114.250928>
- Mazurek, S., Mucciolo, A., Humbel, B. M., & Nawrath, C. (2013). Transmission Fourier transform infrared microspectroscopy allows simultaneous assessment of cutin and cell-wall polysaccharides of *Arabidopsis* petals. *The Plant Journal*, 74, 880–891. <https://doi.org/10.1111/tpj.12164>
- Mouille, G., Ralet, M. C., Cavellier, C., Eland, C., Effroy, D., Hématy, K., McCartney, L., Truong, H. N., Gaudon, V., Thibault, J. F., Marchant, A., & Höfte, H. (2007). Homogalacturonan synthesis in *Arabidopsis thaliana* requires a Golgi-localized protein with a putative methyltransferase domain. *The Plant Journal*, 50, 605–614. <https://doi.org/10.1111/j.1365-313X.2007.03086.x>
- Mouille, G., Robin, S., Lecomte, M., Pagant, S., & Höfte, H. (2003). Classification and identification of *Arabidopsis* cell wall mutants using Fourier-Transform InfraRed (FT-IR) microspectroscopy. *The Plant Journal*, 35, 393–404. <https://doi.org/10.1046/j.1365-313X.2003.01807.x>
- Mravec, J., Guo, X., Hansen, A. R., Schückel, J., Kračun, S. K., Mikkelsen, M. D., Mouille, G., Johansen, I. E., Ulvskov, P., Domozych, D. S., & Willats, W. G. T. (2017). Pea border cell maturation and release involve complex cell wall structural dynamics. *Plant Physiology*, 174, 1051–1066. <https://doi.org/10.1104/pp.16.00097>
- Nguema-Ona, E., Vicié, M., Gotté, M., Plancot, B., Lerouge, P., Bardor, M., & Driouich, A. (2014). Cell wall O-glycoproteins and N-glycoproteins: Aspects of biosynthesis and function. *Frontiers in Plant Science*, 5, 1–12. <https://doi.org/10.3389/fpls.2014.00499>
- Oh, E., Zhu, J. Y., & Wang, Z. Y. (2012). Interaction between BZR1 and PIF4 integrates brassinosteroid and environmental responses. *Nature Cell Biology*, 14, 802–809. <https://doi.org/10.1038/ncb2545>
- Pauly, M., & Keegstra, K. (2016). Biosynthesis of the plant cell wall matrix polysaccharide xyloglucan. *Annual Review of Plant Biology*, 67, 235–259. <https://doi.org/10.1146/annurev-arplant-043015-112222>
- Peaucelle, A., Braybrook, S. A., Le Guillou, L., Bron, E., Kuhlemeier, C., & Höfte, H. (2011). Pectin-induced changes in cell wall mechanics underlie organ initiation in *Arabidopsis*. *Current Biology*, 21, 1720–1726. <https://doi.org/10.1016/j.cub.2011.08.057>
- Peaucelle, A., Louvet, R., Johansen, J. N., Höfte, H., Laufs, P., Pelloux, J., & Mouille, G. (2008). *Arabidopsis phyllotaxis* is controlled by the methyl-esterification status of cell-wall pectins. *Current Biology*, 18, 1943–1948. <https://doi.org/10.1016/j.cub.2008.10.065>
- Peaucelle, A., Wightman, R., & Höfte, H. (2015). The control of growth symmetry breaking in the *Arabidopsis* hypocotyl. *Current Biology*, 25, 1746–1752. <https://doi.org/10.1016/j.cub.2015.05.022>



- Pedmale, U. V., Huang, S. S. C., Zander, M., Cole, B. J., Hetzel, J., Ljung, K., Reis, P. A. B., Sridevi, P., Nito, K., Nery, J. R., Ecker, J. R., & Chory, J. (2016). Cryptochromes interact directly with PIFs to control plant growth in limiting blue light. *Cell*, *164*, 233–245. <https://doi.org/10.1016/j.cell.2015.12.018>
- Pelletier, S., Van Orden, J., Wolf, S., Vissenberg, K., Delacourt, J., Ndong, Y. A., Pelloux, J., Bischoff, V., Urbain, A., Mouille, G., et al. (2010). A role for pectin de-methylesterification in a developmentally regulated growth acceleration in dark-grown *Arabidopsis* hypocotyls. *The New Phytologist*, *188*, 726–739. <https://doi.org/10.1111/j.1469-8137.2010.03409.x>
- Pierik, R., & De Wit, M. (2014). Shade avoidance: Phytochrome signalling and other aboveground neighbour detection cues. *Journal of Experimental Botany*, *65*, 2815–2824. <https://doi.org/10.1093/jxb/ert389>
- Procko, C., Crenshaw, C. M., Ljung, K., Noel, J. P., & Chory, J. (2014). Cotyledon-generated auxin is required for shade-induced hypocotyl growth in *Brassica rapa*. *Plant Physiology*, *165*, 1285–1301. <https://doi.org/10.1104/pp.114.241844>
- Pucciariello, O., Legris, M., Costigliolo, C., José, M., Esteban, C., Dezar, C., Vazquez, M., Yanovsky, M. J., Finlayson, S. A., Prat, S., et al. (2018). Rewiring of auxin signaling under persistent shade. *Proceedings of the National Academy of Sciences*, *115*, 2–7. <https://doi.org/10.1073/pnas.1721110115>
- Robinson, S., Huflejt, M., Barbier de Reuille, P., Braybrook, S. A., Schorderet, M., Reinhardt, D., & Kuhlemeier, C. (2017). An automated confocal micro-extensometer enables in vivo quantification of mechanical properties with cellular resolution. *Plant Cell*, *29*, 2959–2973.
- Rui, Y., Xiao, C., Yi, H., Kandemir, B., Wang, J. Z., Puri, V. M., & Anderson, C. T. (2017). POLYGALACTURONASE INVOLVED IN EXPANSION3 functions in seedling development, rosette growth, and stomatal dynamics in *Arabidopsis thaliana*. *Plant Cell*, *29*, 2413–2432. <https://doi.org/10.1105/tpc.17.00568>
- Sasidharan, R., Chinnappa, C. C., Staal, M., Elzenga, J. T. M., Yokoyama, R., Nishitani, K., Voesenek, L. A. C. J., & Pierik, R. (2010). Light quality-mediated petiole elongation in *Arabidopsis* during shade avoidance involves cell wall modification by xyloglucan endotransglucosylase/hydrolases. *Plant Physiology*, *154*, 978–990. <https://doi.org/10.1104/pp.110.162057>
- Sasidharan, R., Chinnappa, C. C., Voesenek, L. A. C. J., & Pierik, R. (2008). The regulation of cell wall extensibility during shade avoidance: A study using two contrasting ecotypes of *Stellaria longipes*. *Plant Physiology*, *148*, 1557–1569. <https://doi.org/10.1104/pp.108.125518>
- Sasidharan, R., & Pierik, R. (2010). Cell wall modification involving XTHs controls phytochrome-mediated petiole elongation in *Arabidopsis thaliana*. *Plant Signaling & Behavior*, *5*, 1491–1492. <https://doi.org/10.4161/psb.5.11.13643>
- Sénéchal, F., Graff, L., Surcouf, O., Marcelo, P., Rayon, C., Bouton, S., Mareck, A., Mouille, G., Stintzi, A., Höfte, H., Lerouge, P., Schaller, A., & Pelloux, J. (2014). *Arabidopsis* PECTIN METHYLESTERASE17 is co-expressed with and processed by SBT3.5, a subtilisin-like serine protease. *Annals of Botany*, *114*, 1161–1175. <https://doi.org/10.1093/aob/mcu035>
- Sénéchal, F., Wattier, C., Rustérucchi, C., & Pelloux, J. (2014). Homogalacturonan-modifying enzymes: Structure, expression, and roles in plants. *Journal of Experimental Botany*, *65*, 5125–5160. <https://doi.org/10.1093/jxb/eru272>
- Showalter, A. M., & Basu, D. (2016). Extensin and arabinogalactan-protein biosynthesis: Glycosyltransferases, research challenges, and biosensors. *Frontiers in Plant Science*, *7*, 1–9.
- Szymanska-Chargot, M., & Zdunek, A. (2013). Use of FT-IR spectra and PCA to the bulk characterization of cell wall residues of fruits and vegetables along a fraction process. *Food Biophysics*, *8*, 29–42. <https://doi.org/10.1007/s11483-012-9279-7>
- Wang, H., Guo, Y., Lv, F., Zhu, H., Wu, S., Jiang, Y., Li, F., Zhou, B., Guo, W., & Zhang, T. (2010). The essential role of GhPEL gene, encoding a pectate lyase, in cell wall loosening by depolymerization of the de-esterified pectin during fiber elongation in cotton. *Plant Molecular Biology*, *72*, 397–406. <https://doi.org/10.1007/s11103-009-9578-7>
- Wang, X., Wilson, L., & Cosgrove, D. J. (2020). Pectin methylesterase selectively softens the onion epidermal wall yet reduces acid-induced creep. *Journal of Experimental Botany*, *71*, 2629–2640. <https://doi.org/10.1093/jxb/eraa059>
- Wilson, R. H., Smith, A. C., Kac, M., Saunders, P. K., Wellner, N., & Waldron, K. W. (2000). The mechanical properties and molecular dynamics of plant cell wall polysaccharides studied by Fourier-transform infrared spectroscopy. *Plant Physiology*, *124*, 397–405. <https://doi.org/10.1104/pp.124.1.397>
- Wolf, S., Hématy, K., & Höfte, H. (2012). Growth control and cell wall signaling in plants. *Annual Review of Plant Biology*, *63*, 381–407. <https://doi.org/10.1146/annurev-arplant-042811-105449>
- Wolf, S., Mravec, J., Greiner, S., Mouille, G., & Höfte, H. (2012). Plant cell wall homeostasis is mediated by brassinosteroid feedback signaling. *Current Biology*, *22*, 1732–1737. <https://doi.org/10.1016/j.cub.2012.07.036>
- Xiao, C., Somerville, C., & Anderson, C. T. (2014). POLYGALACTURONASE INVOLVED IN EXPANSION1 functions in cell elongation and flower development in *Arabidopsis*. *Plant Cell*, *26*, 1018–1035. <https://doi.org/10.1105/tpc.114.123968>

## SUPPORTING INFORMATION

Additional supporting information can be found online in the Supporting Information section at the end of this article.

**How to cite this article:** Sénéchal, F., Robinson, S., Van Schaik, E., Trévisan, M., Saxena, P., Reinhardt, D., & Fankhauser, C. (2024). Pectin methylesterification state and cell wall mechanical properties contribute to neighbor proximity-induced hypocotyl growth in *Arabidopsis*. *Plant Direct*, *8*(4), e584. <https://doi.org/10.1002/pld3.584>